Jpn. J. Appl. Phys. Vol. 37 (1998) pp. 560–570
Part 1, No. 2, February 1998

Fundamental Limitations to the Viewing Angle of Liquid Crystal Displays with Birefringent Compensators

S. STALLINGA*, J. M. A. van den EERENBEEMD and J. A. M. M. van HAAREN
Philips Research Laboratories, Prof. Holstlaan 4, 5656 AA Eindhoven, The Netherlands

(Received July 17, 1997; accepted for publication November 26, 1997)

The limited viewing angle of twisted nematic (TN) active matrix liquid crystal displays is a major problem for applications in *e.g.* desk-top monitors. The range of viewing angles with acceptably displayed images can be extended by adding birefringent compensation layers to the display. Here it is shown that there are fundamental limitations to the viewing angle range that can be achieved in this way. It may turn out for a particular viewing angle that, (a) grey scale inversion cannot be remedied, and (b) increase of contrast leads to decrease of brightness. The existence of these limitations can be proven by analyzing the change in polarization of light propagating through the display. The vertical viewing angle range of the TN-effect suffers from both limitations. These limitations do leave significant room for improvement by using compensators. The horizontal viewing angle range is not fundamentally limited at all.

KEYWORDS: liquid crystal display, twisted nematic, viewing angle, birefringent compensator

1. Introduction

The twisted nematic (TN) effect[1] is the commonly used liquid crystal effect in active matrix liquid crystal displays (AM-LCDs). One of the major problems of the TN-effect is the strong dependence of the transmission voltage curve on the viewing angle. This leads to optical artefacts, such as loss of contrast, inversion of grey levels and shift of colours, that severely limit the range of viewing angles with acceptable image quality. In the light of the expanding range of applications of AM-LCDs, *e.g.* desk-top monitors, the viewing angle problem becomes increasingly important.

There are several solutions to improve the dependence on viewing angle. One of the prominent solutions is the addition of birefringent layers to the LCD. These layers can be placed between the liquid crystal layer and the analyzer and/or between the polarizer and the liquid crystal layer. Recently, a birefringent viewing angle compensator based on discotic liquid crystalline polymers has been demonstrated.[2,3] Compensator structures based on nematic liquid crystalline polymers,[4] or anorganic birefringent materials[5] also improve the viewing angle dependency substantially. Alternative liquid crystal effects for which relatively simple compensator structures would be sufficient are considered as well. Even liquid crystal effects that have good viewing angle dependency without using compensators have been demonstrated. Such in-cell solutions are the in-plane switching effect,[6–8] the dual-domain, four-domain and multidomain TN-effect,[9,10] the axial-symmetric aligned microcell,[11,12] the vertically aligned nematic effect,[13] and the optically compensated birefringence effect.[14] A completely different approach is based on collimating the light that is incident on the LCD, and scattering the light that leaves the LCD.[15]

At present it is not clear to what extent the viewing angle dependency problem can be solved using birefringent compensators. Knowledge of possible limitations of compensation technology can be quite helpful in the research and development of birefringent compensators, as well as in the comparison of the various wide viewing angle approaches. The question of fundamental limitations of compensation technology is the subject of this paper.

*E-mail address: stalling@natlab.research.philips.com

In order to provide the reader with an elementary understanding of the viewing angle dependency problem, we will first describe the viewing angle artefacts of the TN-effect, and present a qualitative explanation for the viewing angle dependency. The artefacts are:

(i) Loss of contrast. The contrast varies considerably with viewing angle, because the transmission of obliquely incident light in the state addressed with the maximum voltage deviates substantially from zero, as is shown in Fig. 1. This light leakage is due to the angular dependence of the birefringence of the liquid crystal layer.

(ii) Loss of grey level linearity. For normal incidence the transmission decreases monotonically as a function of voltage. This relates the different grey tones to the different values for the applied voltage. For oblique incidence the transmission-voltage curve is quite different, leading to a distorted non-linear spacing of the different grey levels. For a large section of the viewing angles the transmission-voltage curve is even non-monotonical, i.e. a minimum appears. This means that driven states with voltages higher than this minimum look brighter than the minimum transmission state. Consequently, the order of the grey levels is inverted, as is is shown in Fig. 1.

(iii) Loss of colour fidelity. Colours appear less saturated for oblique directions of view. This is caused by obliquely incident light leaking through the pixels addressed with the maximum voltage, i.e. it is related to the low contrast at oblique directions of view. An additional cause of decolouration is the combined wavelength and viewing angle dependence of the transmission.

Starting point of the qualitative explanation is the assumption that the optical transmission is determined by the midplane director alone. Within this simplified picture the liquid crystal is regarded as a uniform birefringent layer with its main optical axis along the midplane director (see Fig 2). Then the birefringence is small for light rays traversing the liquid crystal in a direction nearly parallel to the midplane director (negative vertical viewing angles). On the other hand, the birefringence is large for light rays traversing the liquid crystal in a direction nearly perpendicular to the midplane director (positive vertical viewing angles). For that reason, the polarization of the light rays is hardly changed in the first case, wheras it is substantially changed in the second case.

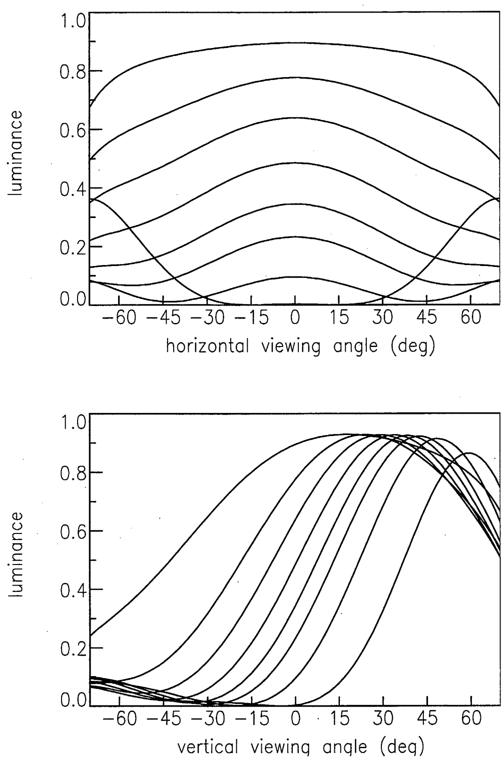

Fig. 1. Calculated luminance for 8 grey levels as a function of horizontal (up) and vertical (down) viewing angle for the TN-effect. The midplane director is in the plane of the (negative) vertical viewing angles (six o'clock display). The cell is filled with the material ZLI 4792 of E. Merck, Darmstadt (Germany) (splay, twist and bend elastic constants are 13.2 pN, 6.6 pN, and 18.3 pN, parallel and perpendicular dielectric constants are 8.3 and 3.1, ordinary and extraordinary refractive indices are 1.48 and 1.58). The cell has a cell-gap of 4.5 μm and a pretilt of 3°, and the polarizers are placed perpendicular to the adjacent rubbing directions. The grey levels, in order of decreasing luminance at normal incidence, correspond to the voltages 1.9 V, 2.2 V, 2.4 V, 2.6 V, 2.8 V, 3.0 V, 3.4 V and 5.0 V.

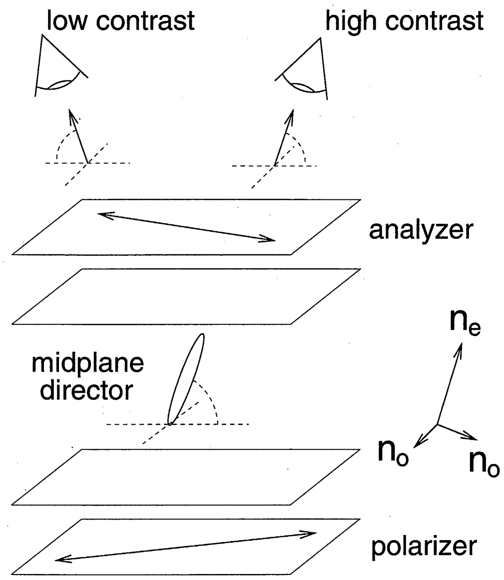

Fig. 2. Simplified picture of contrast variation in the plane of vertical viewing angles.

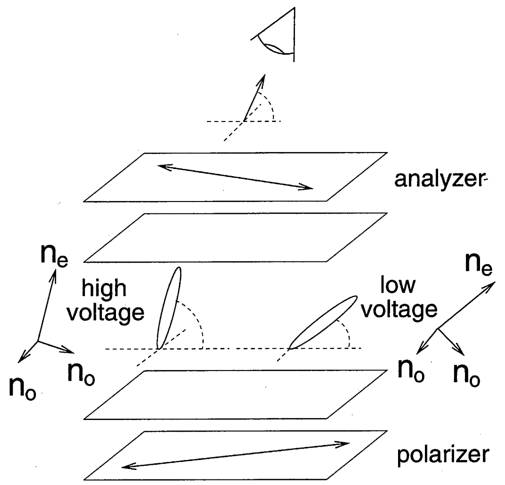

Fig. 3. Simplified picture of grey scale inversion in the plane of negative vertical viewing angles.

As the liquid crystal is placed between crossed polarizers, the display has a relatively dark appearance for negative vertical viewing angles, and a relatively bright appearance for positive vertical viewing angles. This explains the asymmetry between positive vertical viewing angles with low contrast, and negative vertical viewing angles with high contrast. Furthermore, as the tilt of the midplane director increases with voltage, there is a specific voltage for each negative vertical viewing angle, for which the midplane director is parallel to the direction in which the light rays traverse the liquid crystal. In that case the birefringence is minimal (see Fig. 3). This implies that the transmission as a function of voltage has a minimum for this specific voltage. Consequently, there is grey scale inversion for these viewing angles.

The content of this paper is as follows. In §2 it is shown that liquid crystal effects, such as the TN-effect, can be tested for fundamental limitations of the viewing angle. It can be proven whether grey scale inversion is necessarily present or curable in principle by suitably designed compensators. Furthermore, it can be shown whether high brightness and high contrast are compatible or not. The theory underlying these tests is explained in §3. The tests are applied to the TN-effect in §4 using numerical calculations. It is shown that there are limits to the vertical viewing angle range that can be accomplished with compensators. However, these limitations do leave room for improvement of the uncompensated TN-effect. The horizontal viewing angle range is not fundamentally limited, i.e. suitably designed compensators can extend the horizontal viewing angle range to given specifications. The outcomes of the numerical calculations are compared with experimental results in §5. A summary and conclusion is given in §6.

2. Tests for Fundamental Viewing Angle Limitations

2.1 *Qualitative treatment*

The sought-for tests for viewing angle limitations emerge from a detailed analysis of the optics of the TN-effect and of birefringent compensators. The optics of the TN-effect is mainly concerned with the polarization of the light passing through the liquid crystal layer. For normally incident light the description is fairly simple. To a good approximation, the linearly polarized light incident on the liquid crystal layer undergoes a net rotation over 90° in the undriven state of the liquid crystal layer, whereas it remains unchanged in the driven state of the liquid crystal layer. By placing the analyzer perpendicular to the polarizer the undriven state will be bright and the driven state will be dark. By driving the liquid crystal with intermediate voltages grey tones can be displayed. This description changes considerably for obliquely incident light. Now the linearly polarized light entering the liquid crystal in the driven state is transfered to elliptically polarized light leaving the liquid crystal layer. As a consequence, the transmission is non-zero for any orientation of the analyzer, meaning that the contrast is lower than for normally incident light. Similarly, the exiting light for the states with intermediate voltages also suffers from this unwanted ellipticity, which leads to changes in the linearity of the grey levels and even to inversion of the grey levels. These artefacts may be remedied by placing suitably designed birefringent layers between the liquid crystal layer and the analyzer. The elliptically polarized light leaving the liquid crystal layer may be transfered by these birefringent layers to light with the correct polarization state. In this way the transmission-voltage curve can be modified such that the optical artefacts related to the viewing angle dependency may be cured. Birefringent layers placed between the polarizer and the liquid crystal layer change the linearly polarized light exiting the polarizer to elliptically polarized light. This may also lead to the correct polarization of the light leaving the liquid crystal layer. In this way additional degrees of freedom to remedy the viewing angle dependency problem are generated.

In some cases it may appear to be impossible to remedy the artefact of grey scale inversion satisfactorily. This can be understood by considering the elliptically polarized light exiting the liquid crystal as a function of voltage. The different voltages across the liquid crystal cell lead to a variation of the elliptical polarization state of the light that has passed the layer. By varying the voltage a wide variety of polarization states is produced. For some directions of view this exit polarization may turn out to be identical for two different voltages V_1 and V_2. As a consequence the transmission through the analyzer for voltage V_1 is equal to the transmission for voltage V_2. This implies that the transmission-voltage curve either has a maximum or a minimum between V_1 and V_2, meaning that the grey levels are inverted in the voltage regime between V_1 and V_2. Birefringent compensation layers placed between the liquid crystal layer and the analyzer cannot remedy this problem: The identical exit polarizations at voltages V_1 and V_2 are indeed changed by the compensation layers, but are necessarily changed in the same way. Clearly, the transmission at V_1 remains equal to the transmission at V_2, independent of possibly present compensators placed between the liquid crystal layer and the analyzer. As a consequence, grey scale inversion is not solved for this direction of view. Figure 4 shows the possible transmission-voltage curves. Optimum suppression of grey scale inversion is achieved when the maximum or minimum transmission value in the region between V_1 and V_2 differs only slightly from $T_1 = T_2$. Then all grey tones in this voltage region are approximately equally dark. Even with such a viewing angle compensator grey scale information is not properly displayed.

Possibly, a solution can be found by placing additional compensation layers between the polarizer and the liquid crystal layer, thereby modifying the polarization of the light entering the liquid crystal layer. However, even this may turn out to be an insufficient measure. It may appear that the identity of the exit polarizations at V_1 and at V_2 is independent of

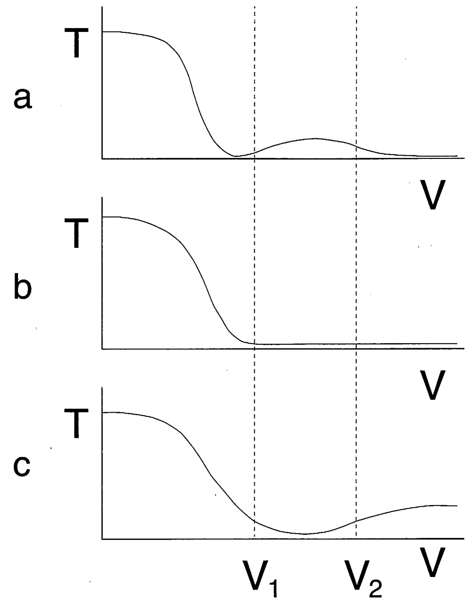

Fig. 4. Possible transmission-voltage curves in case of unavoidable grey scale inversion. In the voltage region between the two voltages V_1 and V_2 for which the retardation difference angle $\beta(V_1, V_2) = 0$ the transmission-voltage curve has a maximum (case a), is flat (case b) or has a minimum (case c).

the entry polarization. Changing the entry polarization will then not help to make the transmission at V_1 different from the transmission at V_2. In such a case, grey scale inversion cannot be avoided by the use of birefringent compensators.

Another viewing angle limitation can be expressed as a constraint on the achievable contrast and brightness. In order to have (almost) unity transmission in the bright state and (almost) zero transmission in the dark state, the polarization incident on the analyzer must be linear and parallel to the analyzer transmission axis for the bright state, whereas it must be linear and perpendicular to the analyzer transmission axis for the dark state. Clearly, in this ideal case these two polarizations are orthogonal to each other. For normally incident light, no birefringent compensators are needed to approximate the ideal case. For light traversing the display obliquely, however, the polarizations leaving the liquid crystal layer in its bright state and in its dark state are generally elliptical and non-orthogonal. Birefringent compensation layers may repair the ellipticity of the light, but they cannot transform non-orthogonal entry polarizations to orthogonal exit polarizations. This means that the ideal case with orthogonal polarizations of the light incident on the analyzer for the dark and bright state cannot be accomplished by placing birefingent compensators between the liquid crystal layer and the analyzer. Again, additional compensation layers between the polarizer and the liquid crystal layer are needed. However, if the two liquid crystal exit polarizations remain non-orthogonal, regardless of the polarization of the light entering the liquid crystal layer, then these additional compensation layers cannot ensure both high contrast and high brightness.

The preceding qualitative treatment can be summarized as follows: (i) The necessary type of grey scale inversion is related to the optical equivalence of the liquid crystal layer at two voltages V_1 and V_2. Optical equivalence means that the exit polarization is the same for the two voltages, and that this identity holds independent of the entry polarization. (ii) Incompatibility of contrast and brightness is related to the lack of optical difference between the liquid crystal layer in the bright and dark state. Maximum optical difference is obtained when the exit polarizations for the bright and dark state can be orthogonal to each other, provided that the right entry polarization is selected.

2.2 *Quantitative treatment*

In order to test a liquid crystal effect for these two fundamental limitations a quantitative measure for the optical difference between two different voltage states of the liquid crystal layer is needed. This measure must be zero if and only if (a) the two exit polarizations are identical, and if (b) this equality is independent of the entry polarization. The so-called retardation difference angle $\beta(V_1, V_2)$, which will be defined in §3, is such a measure. It appears that the transmission of light through the display T as a function of applied voltage V (for a given wavelength and viewing angle) satisifies the following inequality involving the difference measure:

$$|T(V_2) - T(V_1)| \leq R \sin[\beta(V_1, V_2)]. \quad (1)$$

Here R is an attenuation coefficient due to reflections at the air/glass interface ($R \approx 0.9$–1.0 for normal incidence, decreasing with polar viewing angle). By definition, $\beta(V_1, V_2)$ does not depend on the polarization changing properties of the birefringent compensation layers that may be present. Therefore inequality (1) holds for all possible compensator configurations. A proof of (1) will be given in §3.

The two important viewing angle limitations discussed previously can be derived quantitatively from the application of the transmission difference theorem (1):

(i) Necessary existence of grey scale inversion. If there are two voltages V_1 and V_2 for which $\beta(V_1, V_2) = 0$ then it must hold that $T_1 = T_2$ for all possible compensator configurations. This corresponds to the same exit polarization state for V_1 as for V_2, for all entry polarization states. If V_1 and V_2 are in the range of addressing voltages for the LCD, grey scale inversion cannot be solved. On the other hand, if such voltages do not exist, grey scale inversion can be remedied in principle by the use of properly designed compensators.

(ii) Compatibility of high contrast and high brightness. When V_1 is taken to be equal to the dark state driving voltage V_{dark} and V_2 to the bright state driving voltage V_{bright}, the transmission difference theorem reads

$$T_{\text{bright}} - T_{\text{dark}} \leq R \sin[\beta(V_{\text{bright}}, V_{\text{dark}})]. \quad (2)$$

High contrast requires a small T_{dark}, whereas high brightness requires a high T_{bright}. In the most advantageous case we would have $T_{\text{dark}} = 0$ and $T_{\text{bright}} = R$. This corresponds to orthogonal exit polarization states for V_{bright} and V_{dark}. If $\beta(V_{\text{bright}}, V_{\text{dark}})$ is substantially smaller than $\pi/2$ it is not possible to have both $T_{\text{dark}} \approx 0$ and $T_{\text{bright}} \approx R$, regardless of possibly present compensators. This means that the deviation of $\beta(V_{\text{bright}}, V_{\text{dark}})$ from $\pi/2$ is a measure for the incompatibility of high contrast and high brightness. If such an incompatibility exists an increase of contrast will lead to a decrease in brightness.

3. Theoretical Background of the Tests

The objective of this section is to provide the reader with the physical and mathematical theory underlying the viewing angle tests. A definition of the optical difference measure and a proof of inequality (1) result from this theoretical exploration. The proof makes use of the extended Jones-calculus and the Poincaré sphere representation of polarization states. These two subjects will be shortly reviewed, followed by the proof of (1).

3.1 *Extended Jones-calculus*

Jones calculus deals with the change in polarization of light that passes a birefringent layer. It was originally conceived for the description of polarization transfer of normally incident light.[16] However, it can also be applied to obliquely incident light.[17–19] Basic to the Jones method is the way in which reflections are treated. Reflections are treated properly by the 4×4 matrix method of Berreman,[20–23] as this method is based directly on Maxwell's equations. Compared to this method, interference of the forwardly propagating wave with the reflected wave is neglected alltogether in the Jones-method. The attenuation of the forwardly propagating wave at interfaces may be taken into account with the Fresnel coefficients.[17,18] This attenuation can be neglected as well when the variations in refractive indices are sufficiently small. It appears that both the differences in refractive indices between the neighbouring birefringent layers and the birefringence of these layers are small. This means that in practice only the Fresnel coefficients for the air/glass interfaces need to be considered. The smallness of the birefringence also entails further approximations.[17,18] Even in this simplified approach, the (extended) Jones-method provides a quantitatively satisfactory description of the propagation of polarized light through liquid crystal displays, i.e. the results are quantitatively similar to the results obtained using the exact Berreman-method.

Some essential mathematical elements of the (extended) Jones-calculus will be shortly described now:

(i) The polarization is expressed by a vector $\mathbf{p}$ with 2 complex components

$$\mathbf{p} = \begin{bmatrix} A_{\text{p}} \\ A_{\text{s}} \end{bmatrix}. \quad (3)$$

with A_{p} and A_{s} the complex amplitudes of the p-polarized wave and the s-polarized wave.

(ii) The dependence of the exit polarization vector of a birefringent layer $\mathbf{f}$ on the input polarization vector of a birefringent layer $\mathbf{i}$ is expressed as

$$\mathbf{f} = J\mathbf{i}, \quad (4)$$

with J the so-called Jones matrix, a 2×2 complex matrix. When absorption can be neglected J can be expressed as:

$$J = \begin{bmatrix} a & b \\ -b^* & a^* \end{bmatrix}, \quad (5)$$

with

$$a = \cos\delta + \sin\delta\cos(2\mu), \quad (6a)$$

$$b = \sin\delta\sin(2\mu)[\sin(2\nu) + i\cos(2\nu)]. \quad (6b)$$

The physical meaning of the angles δ, μ and ν can be understood by considering the polarization vectors:

$$\mathbf{v}_+ = \begin{bmatrix} \cos\mu \exp(-i\nu) \\ \sin\mu \exp(i\nu) \end{bmatrix}, \tag{7a}$$

$$\mathbf{v}_- = \begin{bmatrix} -\sin\mu \exp(-i\nu) \\ \cos\mu \exp(i\nu) \end{bmatrix}. \tag{7b}$$

When light in a polarization state given by $\mathbf{v}_+$ or $\mathbf{v}_-$ passes the birefringent layer, it remains in this polarization state up to a phase factor $\exp(i\delta)$ or $\exp(-i\delta)$, respectively:

$$J\mathbf{v}_+ = \exp(+i\delta)\mathbf{v}_+, \tag{8a}$$

$$J\mathbf{v}_- = \exp(-i\delta)\mathbf{v}_-. \tag{8b}$$

The polarization vectors $\mathbf{v}_+$ and $\mathbf{v}_-$ are called the eigenpolarization vectors of J, and $\exp(i\delta)$ and $\exp(-i\delta)$ are the attendant eigenvalues of J. The angle δ related to these eigenvalues is called the retardation angle of J.

(iii) The Jones matrix J_{LC} of the liquid crystal layer depends explicitly on the viewing angle and the wavelength and implicitly on the voltage via the director profile. The dependence of J_{LC} on these parameters can be calculated in the following way. Divide the liquid crystal layer in N sublayers with approximately constant tilt and twist angles. The Jones matrix J_{LC} can then be written as the product of the N sublayer Jones matrices:

$$J_{\mathrm{LC}} = J_N J_{N-1} \ldots J_2 J_1, \tag{9}$$

An analytical expression for the Jones-matrix of an individual sublayer is given in the Appendix. As mentioned previously, the additional matrices containing the Fresnel-coefficients[17,18] are neglected in this approach. The compensators on both sides of the liquid crystal consist of stacks of birefringent layers. The corresponding Jones matrices $J_{\text{comp,top}}$ and $J_{\text{comp,down}}$ can therefore be calculated in the same way as J_{LC}. The Jones matrix of the total system can then be expressed as the product of the Jones matrices of all the individual components:

$$J = J_{\text{comp,top}} J_{\mathrm{LC}} J_{\text{comp,down}}. \tag{10}$$

(iv) The transmission of the compensated liquid crystal layer placed between two (ideal) polarizers described by transmitted polarization vectors $\mathbf{P}_1$ and $\mathbf{P}_2$ is given by

$$T = R|\mathbf{P}_2^* \cdot (J\mathbf{P}_1)|^2. \tag{11}$$

where R is a coefficient that takes into account the reflections at the air/glass interfaces. An expression for R is given in the appendix. The polarization vectors $\mathbf{P}_1$ and $\mathbf{P}_2$ can be calculated using the so-called equivalent-polarizer model.[24]

3.2 *Poincaré sphere representation*

A convenient and beautiful way to describe polarized light and the change of polarization by birefringent systems makes use of the representation of polarization vectors on the Poincaré sphere.[25–27] A schematic picture of the sphere is shown in Fig. 6. Each point on the Poincaré sphere can be characterized by two angles that also characterize a polarization vector. This means that all polarization states can be mapped onto the sphere. The coordinates of the points on the sphere are called Stokes parameters. They can be expressed as:

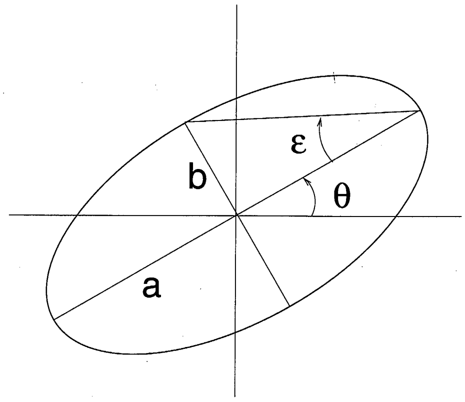

Fig. 5. The polarization ellips is characterized by the ellipticity angle ε ($\tan\varepsilon$ is defined as the ratio between the short axis b and the long axis a of the ellips, and the rotation angle θ (defined as the angle between the long axis of the ellips and a reference axis).

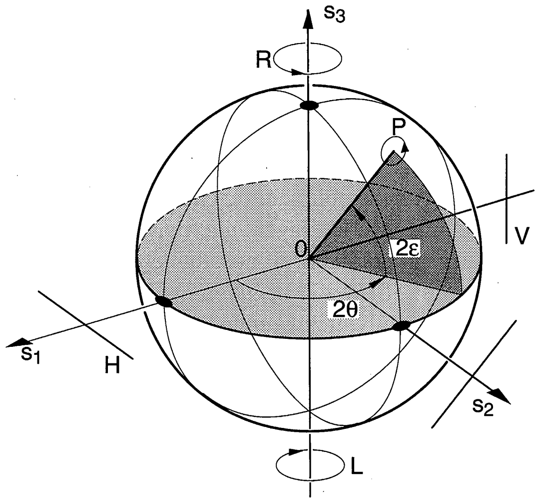

Fig. 6. The Poincaré sphere representing the different polarization states.

$$S_1 = \cos(2\varepsilon)\cos(2\theta), \tag{12a}$$

$$S_2 = \cos(2\varepsilon)\sin(2\theta), \tag{12b}$$

$$S_3 = \sin(2\varepsilon). \tag{12c}$$

The angles ε and θ are the ellipticity angle and the inclination angle, i.e. $\tan\varepsilon$ is equal to the ratio of the short and long axis of the polarization ellips and θ is the angle of the long axis of the polarization ellips (with a reference axis). The polarization ellips is drawn in Fig. 5. The poles of the sphere represent the circularly polarized states, the equator represents the linearly polarized states, and the other points represent the elliptically polarized states.

The action of a Jones matrix J on a polarization vector can be visualized as a rotation over the Poincaré sphere of the Stokes vector representing the polarization vector. The rotation axis intersects the Poincaré sphere in the representation points of the eigenpolarizations $\mathbf{v}_+$ and $\mathbf{v}_-$, and the rotation angle is equal to two times the retardation angle δ.

The inner product between two polarization vectors $\mathbf{i}$ and $\mathbf{f}$ can be visualized using the Poincaré sphere once more . It appears that:

$$|\mathbf{f}^* \cdot \mathbf{i}|^2 = \frac{1}{2} + \frac{1}{2}\mathbf{S}_\mathbf{i} \cdot \mathbf{S}_\mathbf{f} = \cos^2 \eta, \quad (13)$$

with $\mathbf{S}_\mathbf{i}$ and $\mathbf{S}_\mathbf{f}$ the Stokes vectors corresponding to **i** and **f**, and where 2η is the angle between $\mathbf{S}_\mathbf{i}$ and $\mathbf{S}_\mathbf{f}$. When **i** and **f** are two orthogonal polarizations, i.e. when $\mathbf{f}^* \cdot \mathbf{i} = 0$, the angle η equals $\pi/2$, meaning that orthogonal polarization states are represented by points that lie opposite to each other on the Poincaré sphere.

3.3 *Proof of transmission difference theorem*

The transmission difference theorem eq. (1) can now be derived. Consider to that end the transmission coefficients T_1 and T_2 for two different values of the applied voltage V_1 and V_2, respectively, and for one particular viewing angle and wavelength. The Jones matrices of the liquid crystal layer for these two voltages J_1 and J_2 change the polarization of the light entering the liquid crystal $\mathbf{i} = J_{\text{comp,down}}\mathbf{P}_1$ to the exit polarizations $\mathbf{g}_1 = J_1\mathbf{i}$ and $\mathbf{g}_2 = J_2\mathbf{i}$, respectively. The transmission coefficients T_1 and T_2 are found by projecting $\mathbf{g}_1$ and $\mathbf{g}_2$ on $\mathbf{f} = J_{\text{comp,top}}{}^{-1}\mathbf{P}_2$, which leads to:

$$T_1 = R|\mathbf{f}^* \cdot \mathbf{g}_1|^2 = \frac{1}{2}R\left[1 + \mathbf{S}_\mathbf{f} \cdot \mathbf{S}_1\right], \quad (14a)$$

$$T_2 = R|\mathbf{f}^* \cdot \mathbf{g}_2|^2 = \frac{1}{2}R\left[1 + \mathbf{S}_\mathbf{f} \cdot \mathbf{S}_2\right]. \quad (14b)$$

Here eq. (13) is used to express T_1 and T_2 in terms of the Stokes vectors $\mathbf{S}_1$, $\mathbf{S}_2$ and $\mathbf{S}_\mathbf{f}$ corresponding to $\mathbf{g}_1$, $\mathbf{g}_2$ and **f**, respectively. The difference between the transmission coefficients can be written as

$$T_2 - T_1 = \frac{1}{2}R\mathbf{S}_\mathbf{f} \cdot (\mathbf{S}_2 - \mathbf{S}_1). \quad (15)$$

Now it follows that

$$(T_2 - T_1)^2 = \frac{1}{4}R^2\left[\mathbf{S}_\mathbf{f} \cdot (\mathbf{S}_2 - \mathbf{S}_1)\right]^2 \le \frac{1}{4}R^2|\mathbf{S}_\mathbf{f}|^2\,|\mathbf{S}_2 - \mathbf{S}_1|^2. \quad (16)$$

Because Stokes vectors are unit vectors, it is found that

$$|\mathbf{S}_\mathbf{f}|^2 = 1, \quad (17a)$$

$$\begin{aligned}|\mathbf{S}_2 - \mathbf{S}_1|^2 &= \mathbf{S}_2{}^2 - 2\mathbf{S}_2 \cdot \mathbf{S}_1 + \mathbf{S}_1{}^2 \\ &= 2\left[1 - \mathbf{S}_2 \cdot \mathbf{S}_1\right] \\ &= 2\left[1 - \cos(2\eta)\right] \\ &= 4\sin^2\eta, \end{aligned} \quad (17b)$$

where 2η is the angle between $\mathbf{S}_1$ and $\mathbf{S}_2$. Consequently, the transmission difference satisfies the following inequality:

$$|T_2 - T_1| \le R\sin\eta. \quad (18)$$

It appears that the range of values taken by η is limited. This can be seen by considering the relation between $\mathbf{g}_1$ and $\mathbf{g}_2$:

$$\mathbf{g}_2 = J_2 J_1{}^{-1}\mathbf{g}_1. \quad (19)$$

The Jones matrix $J_2 J_1{}^{-1}$ is related to a rotation on the Poincaré sphere. Applying this rotation to the Stokes vector $\mathbf{S}_1$ results in the Stokes vector $\mathbf{S}_2$, as shown in Fig. 7. The retardation angle β of $J_2 J_1{}^{-1}$ is called the retardation difference angle of J_1 and J_2. This angle is the optical difference measure introduced in the §2. It equals zero if and only if

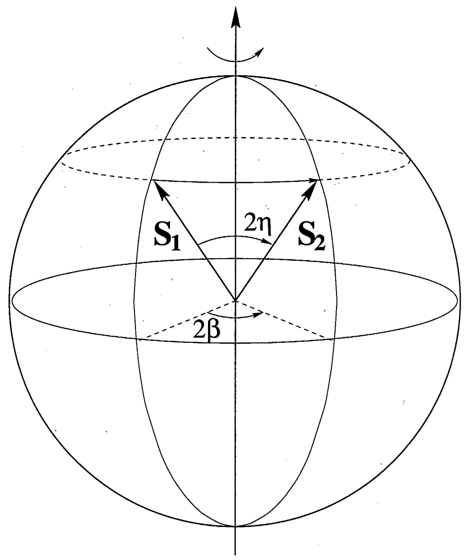

Fig. 7. The Stokes vectors $\mathbf{S}_1$ and $\mathbf{S}_2$ point to the representation points of the polarization states at the exit of the liquid crystal layer for the two voltages. The rotation relating $\mathbf{S}_1$ and $\mathbf{S}_2$ corresponds to the Jones matrix $J_2 J_1{}^{-1}$. The rotation angle is twice the retardation angle β. For the sake of clarity, the eigenpolarizations of $J_2 J_1{}^{-1}$ are mapped onto the poles of the Poincaré sphere in this figure.

$J_1 = J_2$, i.e. if the liquid crystal is optically equivalent at the two voltages. On the other hand, β is equal to $\pi/2$ when the optical difference between the two voltage states is maximal. It appears from Fig. 7 that the angle 2η between $\mathbf{S}_1$ and $\mathbf{S}_2$ can not take any value. As the latitude of $\mathbf{S}_1$ and $\mathbf{S}_2$ can vary from $\pi/2$ to 0, 2η can vary from 0 to 2β in case $\beta < \pi/2$ and from 0 to $2\pi - 2\beta$ in case $\beta > \pi/2$. It follows that η satisfies

$$\sin\eta \le \sin\beta. \quad (20)$$

This finally leads to the transmission difference theorem:

$$|T_2 - T_1| \le R\sin\beta. \quad (21)$$

The retardation difference angle β only depends on the optical properties of the liquid crystal layer, as it is the retardation angle of the Jones matrix $J_2 J_1{}^{-1}$. This independence of the optical properties of the compensation layers implies that the upper limit of the transmission difference in (1) is the same for all possible compensator configurations.

4. Application to the Twisted Nematic Effect

In §2 and §3 we have derived two possible limitations of compensated liquid crystal effects. Depending on the value of the so-called retardation difference angle β as a function of wavelength, viewing angle and voltages V_1 and V_2, it may appear that for a certain direction of view grey scale inversion cannot be avoided or that high contrast and high brightness cannot be achieved simultaneously. Any liquid crystal effect can be tested for these two limitations by numerically calculating the retardation difference angle as a function of wavelength, viewing angle and voltages V_1 and V_2. In the following, the TN-effect is subjected to these tests.

4.1 *Grey scale inversion*

In order to test if grey scale inversion can be avoided in principle, the retardation difference angle $\beta(V_1, V_2)$ is calculated numerically for a range of voltages V_1 and V_2. Figure 8

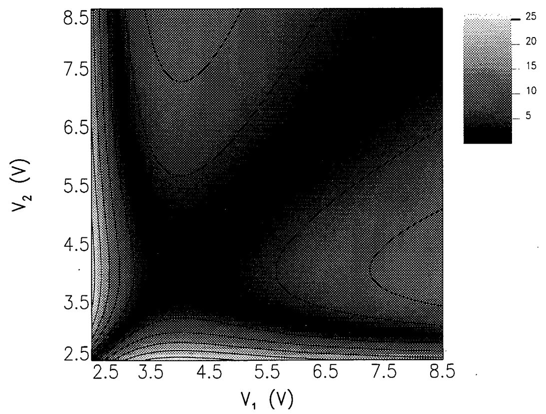

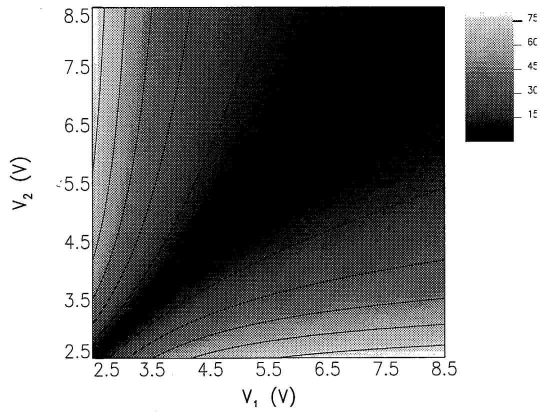

Fig. 8. Contour plot of the retardation difference angle as a function of the voltages V_1 and V_2 for 546 nm wavelength and 30° negative vertical viewing angle (left) and 50° horizontal viewing angle (right). The occurence of grey scale inversion that can not be completely remedied with compensation layers is reflected in the fork-like structure of the left diagram.

shows the result of the calculations for 30° (negative) vertical viewing angle and 50° horizontal viewing angle. Both viewing angles give rise to grey scale inversion for the uncompensated TN-effect (see Fig. 1). In the calculation we have assumed a 4.5 μm thick, 90° twist cell with a pretilt angle of 2.5°, filled with the material ZLI 4792 from E. Merck, Darmstadt (Germany), the wavelength was taken to be 546 nm (green). Data concerning material parameters were obtained from the supplier (the elastic constants for splay, twist and bend are 13.2 pN, 6.6 pN and 18.3 pN, respectively, the perpendicular and parallel dielectric constants are 3.1 and 8.3, respectively, and the ordinary and extraordinary refractive indices are 1.48 and 1.58, respectively).

The left diagram of Fig. 8, pertaining to the vertical viewing angle with grey scale inversion, has two dark lines that intersect at the voltage V_b = 4.0 V. The dark line along the diagonal is due to the fact that $\beta(V, V) \equiv 0$ for all V. Along the curved off-diagonal dark line the retardation difference angle is approximately zero. It appears that β is identically zero at a single point on this line given by the voltages V_1^{gsi} = 3.1 V and V_2^{gsi} = 6.5 V. This means that the liquid cystal layer is optically equivalent for these two voltages (for the specific viewing angle and wavelength under consideration). Clearly, grey scale inversion cannot be avoided for this viewing angle and wavelength.

The voltages V_1^{gsi} = 3.1 V, V_b = 4.0 V and V_2^{gsi} = 6.5 V correspond to tilt angles of the midplane director equal to 62°, 76° and 88°, respectively. According to the qualitative explanation of grey scale inversion given in the introduction (see Fig. 3), the minimum in the transmission voltage curve occurs when the light ray travels along the midplane director. According to Snel's law a 30° viewing angle then corresponds to a midplane tilt angle equal to $90° - \arcsin\{\sin(30°)/1.5\} = 71°$ for the minimum in the transmission voltage curve. This is in the grey scale inversion regime between V_1^{gsi} and V_2^{gsi}. Clearly, there is qualitative agreement between the simple picture of grey scale inversion and the more refined calculations of this paper.

The characteristic fork-like structure of the left diagram of Fig. 8 was observed for all (negative) vertical viewing angles. The intersection voltage V_b and the voltages V_1^{gsi} and V_2^{gsi} for which $T(V_1^{gsi}) \equiv T(V_2^{gsi})$ increase with decreasing polar viewing angle, going to infinity when the polar viewing angle reaches zero. Figure 9 shows these voltages as a function of the polar viewing angle. When the maximum driving voltage V_{max} is smaller than V_1^{gsi} there is no grey scale inversion limitation. According to Fig. 9 this is the case for polar viewing angles smaller than approximately 10° when V_{max} = 5.0 V is chosen.

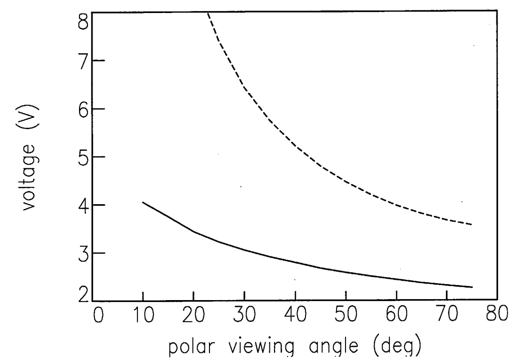

Fig. 9. The voltages V_1^{gsi} (full line) and V_2^{gsi} (dashed line) as a function of polar viewing angle in the negative vertical viewing angle plane.

As to the dependence on wavelength, the calculated retardation difference angles hardly change when the wavelength is varied over the visible spectrum. Consequently, the voltages V_1^{gsi}, V_2^{gsi} and V_b have no significant dependence on wavelength. This also implies that these voltages are relatively independent of the liquid crystal layer thickness d, since all optical properties depend on the ratio $d\Delta n/\lambda$, not on the variables d and λ independently, provided that Δn is sufficiently small. This is not surprising in view of the qualitative explanation of grey scale inversion given in the introduction. In this simplified picture only the angle between the direction of view and the midplane director is relevant, not the wavelength of the passing light or the cell-gap.

Grey scale inversion voltages V_1^{gsi} and V_2^{gsi} can also be found for positive vertical viewing angles. Here, however, they are close to the threshold voltage. This means that the bright states are inverted. Fortunately, the human visual system is not very sensitive to this kind of grey scale inversion. The voltages V_1^{gsi} and V_2^{gsi} both increase with increasing polar viewing angle. As a consequence, this grey scale inversion may shift to the mid-grey levels for the larger polar viewing

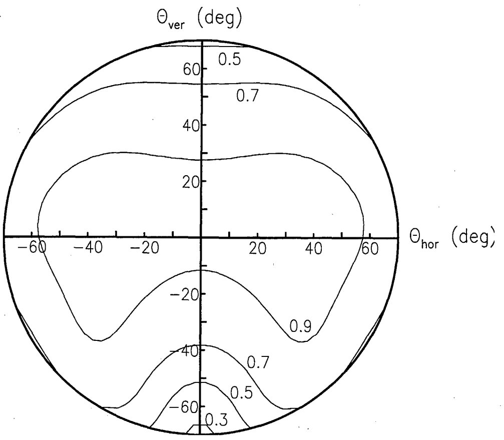

Fig. 10. Contour plots of the maximum transmission difference between the black and white state (at 5.0 V and 1.9 V, respectively) as a function of horizontal viewing angle $\theta_{\rm hor}$ and vertical viewing angle $\theta_{\rm ver}$ for 546 nm wavelength light.

angles.

The right diagram of Fig. 8, pertaining to the horizontal viewing angle with grey scale inversion, does not have the characteristic fork-like structure of the diagrams for the (negative) vertical viewing angles. As a consequence, two different voltages $V_1^{\rm gsi}$ and $V_2^{\rm gsi}$ for which $\beta(V_1^{\rm gsi}, V_2^{\rm gsi}) = 0$ do not exist. This indicates that the inversion of grey levels for these directions of view can be remedied by properly designed compensators. A cross-over from incurable to curable grey scale inversion occurs for the intermediate diagonal viewing angles.

4.2 *Contrast and brightness*

The compatibility of contrast and brightness is tested by calculating the retardation difference angle $\beta(V_{\rm min}, V_{\rm max})$ for a range of viewing angles and for a selected wavelength (λ = 546 nm). Figure 10 shows the resulting maximum transmission difference $R\sin[\beta(V_{\rm min}, V_{\rm max})]$ for $V_{\rm min}$ = 1.9 V and $V_{\rm max}$ = 5.0 V. For all horizontal viewing angles the maximum transmission difference between the white and black state is quite close to the maximum, meaning that both a high brightness and a high contrast can be achieved, provided that proper compensation foils are added to the display. For both positive and negative vertical viewing angles, however, the maximum transmission difference between the white and black state is substantially smaller than R, meaning that high contrast and high brightness are incompatible for these viewing angles. This is in agreement with the characteristics of the uncompensated TN-effect. In the region of high contrast (negative vertical viewing angles) the brightness is relatively low, whereas in the region of low contrast (positive vertical viewing angles) the brightness is relatively high (see Fig. 1). Addition of birefringent compensation layers in order to extend the vertical contrast range will consequently lead to a decrease in brightness.

5. Experiment

5.1 *Experimental considerations*

The results of §4 concerning the grey scale inversion limitation can be compared to experiment in the following way. The two parameters describing the polarization of the light exiting the liquid crystal layer, *e.g.* the ellipticity angle ε and the inclination angle θ (see Fig. 5), are measured as a function of voltage. When the resulting curve in the $\varepsilon - \theta$ plane has a loop, there are two voltages V_1 and V_2 for which the exit polarization states are identical. These voltages correspond to the point where the curve intersects itself. The occurence of such a loop entails two important aspects. The first aspect deals with the exit polarization for the entry polarization orthogonal to the original one. According to theory, orthogonal entry polarizations lead to orthogonal exit polarizations. This means that an $\varepsilon - \theta$ curve similar to the first one can be expected. The value for the ellipticity angle ε has the opposite sign and the value for the inclination angle θ differs 90°. In particular, the two voltages V_1 and V_2 corresponding to the intersection point in the exit polarization curves are the same. The second aspect is related to the polarization vectors $\mathbf{g}_1^{\pm}$ and $\mathbf{g}_2^{\pm}$ at V_1 and V_2, respectively. Here '+' and '−' stand for the two orthogonal entry polarization vectors $\mathbf{f}^+$ and $\mathbf{f}^-$. Experimentally, the loop in the $\varepsilon - \theta$ curve implies that the polarization vectors $\mathbf{g}_1^{\pm}$ and $\mathbf{g}_2^{\pm}$ are equal up to a phase factor, i.e.

$$\mathbf{g}_1^{\pm} = \exp\left(i\phi^{\pm}\right)\mathbf{g}_2^{\pm}. \tag{22}$$

If the phase factors ϕ^+ and ϕ^- are equal to each other, the optical equivalence of the liquid crystal layer at V_1 and V_2 is established. This can be seen as follows. Consider an entry polarization vector $\alpha\mathbf{f}^+ + \beta\mathbf{f}^-$. The exit polarization vectors $\mathbf{h}_1$ and $\mathbf{h}_2$ at V_1 and V_2, respectively, will then be the same linear combinations of $\mathbf{g}_1^+$ and $\mathbf{g}_1^-$, and of $\mathbf{g}_2^+$ and $\mathbf{g}_2^-$, i.e.

$$\mathbf{h}_1 = \alpha\mathbf{g}_1^+ + \beta\mathbf{g}_1^-, \tag{23a}$$

$$\mathbf{h}_2 = \alpha\mathbf{g}_2^+ + \beta\mathbf{g}_2^-. \tag{23b}$$

It follows that $\mathbf{h}_1 = \exp(i\phi)\mathbf{h}_2$ if and only if $\phi^+ = \phi^-$. As a consequence, an additional measurement for a third entry polarization is needed in order to test for the equality of the two phase factors. This entry polarization must differ from the two previously considered orthogonal entry polarizations. If a loop in the exit polarization curve is present again, and if the intersection point corresponds to the same two voltages V_1 and V_2 as in the first measurement, the two phase factors are equal. Clearly, measurements for two different non-orthogonal entry polarizations are required to test for the grey scale inversion limitation. In the present experiment a linear and a circular entry polarization are chosen.

The constraint on contrast and brightness is not so easily accessible by experiment as the grey scale inversion limitation. Such an experiment would be quite time-consuming, as it should comprise of the measurement of the exit polarization for the states with minimum and maximum driving voltage for a large number of entry polarizations and for a large number of different viewing angles. Furthermore, it is not straightforward to extract the retardation difference angle from these data. Therefore no experiments concerning this limitation are presented here.

5.2 *Experimental set-up*

The exit polarization is measured using a set-up as shown in Fig. 11. Light from the He–Ne laser (wavelength 632.8 nm) is split into two beams, which are both polarized by a fixed polarizer, with its transmission axis at an angle γ with the plane of incidence. The first beam then passes the liquid crystal cell, mounted on a rotatable stage, and a quarter-wave ($\lambda/4$) plate.

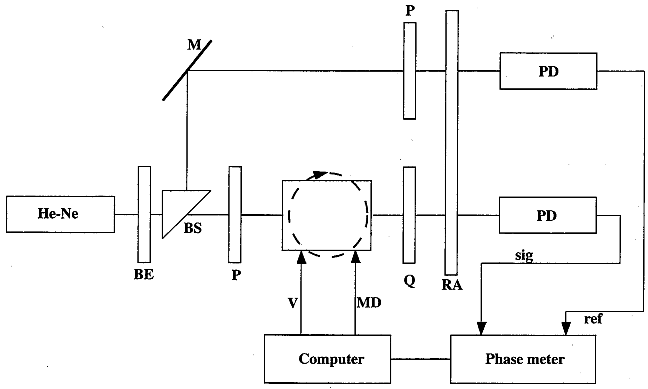

Fig. 11. Block diagram of the measurement setup. He–Ne indicates a He–Ne laser, BE a beam expander, P a fixed polarizer, Q a quarter-wave plate, R.A. a rotating analyzer, PD a photo detector, BS a beam splitter, and M a mirror. The rotation of the liquid crystal cell in the beam and the applied voltage are controlled by a computer.

Finally, both beams pass an analyzer, rotating with angular frequency ω. As a consequence, the photo detector measures an oscillating transmission for the two beams. The phase difference between these oscillating transmission values is measured by the phase meter. The setup described here can also be used to measure the thickness and pretilt angle of a non-twisted liquid crystal cell.[28]

The ellipticity angle ε and the inclination angle θ for the light leaving the liquid crystal can now be determined using the following procedure. First, the orientation of the $\lambda/4$-plate is adjusted such that the amplitude of the oscillating transmssion after the rotating analyzer has its maximum value. In that case the elliptically polarized light exiting the liquid crystal is transformed to linearly polarized light by the $\lambda/4$-plate. This means that the slow axis of the $\lambda/4$-plate is either parallel or perpendicular to the long axis of the polarization ellips. Furthermore, this linear polarization makes an angle $-\varepsilon$ or $+\varepsilon$, respectively, with the long axis of the polarization ellips, i.e. an angle $\theta-\varepsilon$ or $\theta+\varepsilon$ with the plane of incidence. The adjustment procedure for the $\lambda/4$-plate is quite difficult when the light leaving the liquid crystal is nearly circularly polarized, as in that case the variation in the amplitude of the oscillating part of the transmission as a function of the $\lambda/4$-plate orientation is very small. As a consequence, the accuracy of this method is larger for nearly linearly polarized light than for nearly circularly polarized light. After this procedure the phase differences $\Phi_{\parallel}$ and $\Phi_{\perp}$ for the $\lambda/4$-plate slow axis oriented parallel and perpendicular, respectively, to the long axis of the polarization ellips are measured. These two phase differences are then equal to twice the angle between the linear polarization of the reference beam and the linear polarization of the beam after it has passed the $\lambda/4$-plate. This can be expressed by the equations:

$$\Phi_{\parallel} = 2\theta + 2\varepsilon - 2\gamma, \tag{24}$$

$$\Phi_{\perp} = 2\theta - 2\varepsilon - 2\gamma. \tag{25}$$

The wanted angles ε and θ can now be calculated from the measured values of $\Phi_{\parallel}$ and $\Phi_{\perp}$. The accuracy of the method is typically 2° for both ε and θ. The error in θ diverges rapidly for values of $|\varepsilon|$ above approximately 40° (nearly circular polarization).

The liquid crystal cell was filled with the liquid crystal ZLI4792, produced by E. Merck, Darmstadt (Germany). This is the material for which the numerical calculations of §4 have been done. The two substrates of the liquid crystal cell were coated with transparent conductive electrodes and with the polyimide AL 1051, produced by JSR, Kawasaki (Japan).[29] The polyimide layers, with thickness 110 nm, were rubbed to produce a twist angle of 90°. The cell-gap and pretilt angle were determined from a similarly prepared cell with a non-twisted liquid crystal layer using the method of Van Sprang.[28] The measured values were 8.1 μm and 2.5°. All the liquid crystal and cell parameters pertain to a temperature of 20°C. The polarization measurements were also done at a temperature of 20°C. The cell was placed in the beam such that the direction of incidence of the light on the cell corresponds to a direction of view at 40° from the normal in the plane of (negative) vertical viewing angles. According to the numerical calculations of §4, this direction of view gives rise to grey scale inversion that cannot be solved by compensation foils.

5.3 *Experimental results*

Figure 12 shows the measured and calculated angles ε and θ for voltages between 0 and 10 V for the linear entry polarization at 45° with the plane of incidence. This entry polarization is (practically) perpendicular to the rubbing direction at the entry side of the liquid crystal cell, i.e. the polarizer orientation that is most frequently used in practice. Both the measured and the calculated curves clearly show a loop. The agreement between experiment and theory is satisfactory, especially in view of the determination of the large number of relevant parameters (three elastic constants, two dielectric constants, two refractive indices, the cell-gap, the pretilt, the polyimide thickness and dielectric constant) in separate, independent experiments. The two voltages corresponding to the intersection point in the exit polarization curves give rise to equal transmission values. According to numerical calculations these voltages are $V_1 = 2.61$ V and $V_2 = 4.98$ V. The measurements give rise to the values $V_1 = (2.6 \pm 0.1)$ V and $V_2 = (5.0 \pm 0.1)$ V, in good agreement with the calculations.

Figure 13 shows the measured and calculated angles ε and θ for voltages between 0 and 10 V for the right-handed circular entry polarization. Agreement between experiment and theory is again satisfactory, apart from the points close to circular polarization, which have been discarded. This is due to the limited accuracy of the measurement method in this regime. The loop in the exit polarization curve is again clearly present. The intersection voltages are now $V_1 = (2.5 \pm 0.2)$ V and $V_2 = (5.0 \pm 0.2)$ V, in agreement with the previous measurement as well as the numerical calculations. It follows that the experiments support the conclusions obtained from the numerical calculations: Grey scale inversion for the (negative) vertical viewing angles cannot be remedied by adding birefringent compensation foils to the display.

6. Summary and Conclusion

Nowadays the TN-effect is commonly used by all AM-LCD manufacturers. The range of viewing angles with acceptable image quality is considerably narrowed by the loss of contrast, grey scale linearity and colour fidelity. Improvement can be achieved by placing suitably designed birefringent layers between the polarizer and the liquid crystal layer and/or between the liquid crystal layer and the analyzer. This

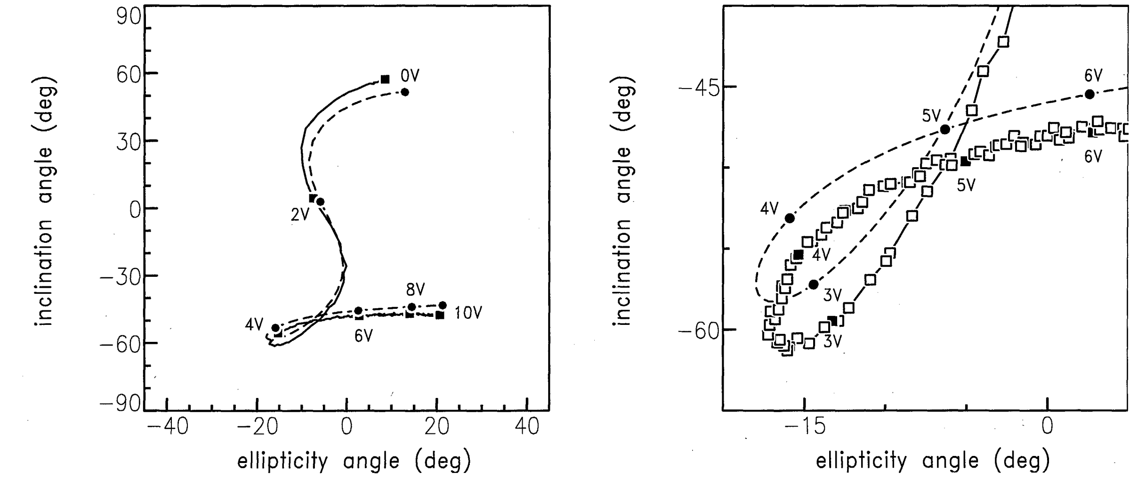

Fig. 12. Measured (full line) and calculated (dashed) ellipticity of 632.8 nm light exiting the twisted nematic layer at an angle of 40° with the normal in the plane of (negative) vertical viewing angles. The filled circles indicate the calculated exit polarizations for a number of selected voltages, the filled squares indicate the corresponding measured exit polarizations. The open squares indicate the other measured exit polarizations. For the sake of clarity, they are only displayed in the inset on the right. The entry polarization was at 45° with the plane of incidence, perpendicular to the rubbing direction at the entry side of the liquid crystal cell.

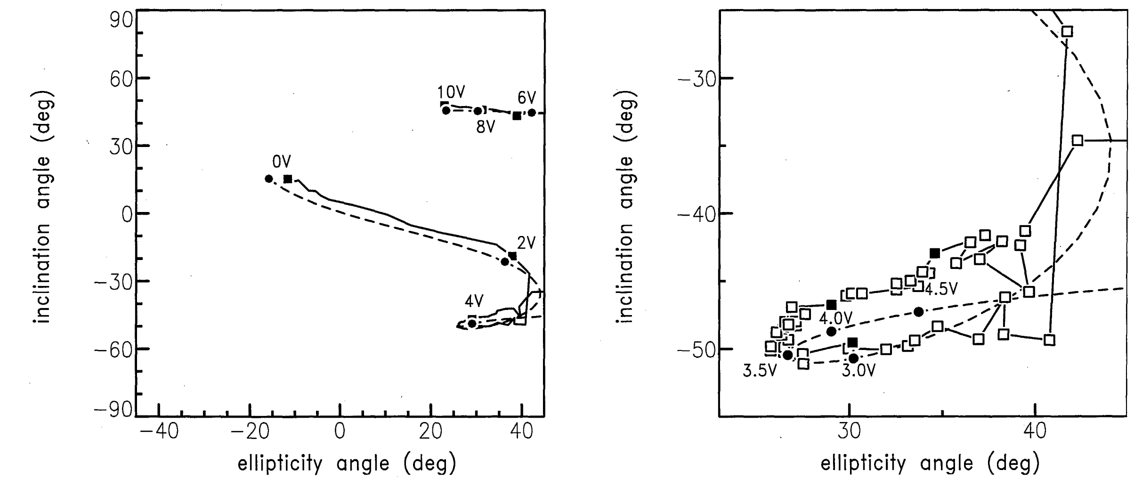

Fig. 13. Measured (full line) and calculated (dashed) ellipticity of 632.8 nm light leaving the twisted nematic layer at an angle of 40° with the normal in the plane of (negative) vertical viewing angles. The filled circles indicate the calculated exit polarizations for a number of selected voltages, the filled squares indicate the corresponding measured exit polarizations. For the sake of clarity, they are only displayed in the inset on the right. The entry polarization was right handed circular.

paper addresses the question to what extent the viewing angle problem of the TN-effect can be solved by birefringent compensators.

It appears that any liquid crystal effect can be tested for two fundamental viewing angle limitations. These tests result from an analysis of the way in which the liquid crystal changes the polarization of passing light. First, it is shown that grey scale inversion (for a certain direction of view) cannot always be solved by birefringent compensators. Second, it is shown that it is not always possible to achieve both high contrast and high brightness (for a certain direction of view) by compensators.

The tests for fundamental viewing angle limitations are applied to the TN-effect using numerical calculations as well as experiments. It is concluded that the vertical viewing angle range is limited in a fundamental way. The grey scale inversion for vertical viewing angles can not be cured by compensators, and contrast can only be improved by compensators at the expense of brightness. Although the vertical viewing angle range is limited, it is quite possible to improve the uncompensated TN-effect substantially. These improvements, as well as the presently discussed limitations, appear clearly from the compensated LCDs that have been demonstrated.[2–5] The horizontal viewing angle range is not fundamentally limited. This means that suitably designed compensators can solve grey scale inversion completely and can give rise to both a high contrast ratio and high brightness.

Acknowledgements

We thank Peter van de Witte for helpful discussions and ideas, and Gerda van de Spijker for providing us with the liquid crystal cells.

Appendix

The numerical calculation of the display transmission using the extended Jones-method requires a way to calculate the Jones-matrix of a uniform birefringent layer. An analytical expression for this Jones-matrix can be derived within the small-birefringence approximation of the extended Jones-method. The Jones-matrix can be expressed, as any Jones-matrix, in terms of the retardation angle and the eigenpolarizations. The eigenpolarization states pertaining to a uniform birefringent layer are linearly polarized. They are called the ordinary wave, with linear polarization along **o**, and the extraordinary wave, with linear polarization along **e**. The unit vector of the extraordinary polarization **e** is the unit vector along the projection of the director **n** on the plane perpendicular to the wave vector **k**. The mutually perpendicular unit vectors **e** and **o** make an angle χ with **p** and **s**, the basis vectors in the plane perpendicular to **k**:

$$\mathbf{e} = \cos\chi\mathbf{p} + \sin\chi\mathbf{s}, \qquad \text{(A·1a)}$$

$$\mathbf{o} = -\sin\chi\mathbf{p} + \cos\chi\mathbf{s}, \qquad \text{(A·1b)}$$

The angle χ is related to the polar and azimuthal angles of the optical axis θ and ϕ, respectively, and to the angle of incidence α by

$$\tan\chi = \frac{\cos\theta\sin\phi}{\cos\alpha\,\cos\theta\,\cos\phi - \sin\alpha\,\sin\theta}. \qquad \text{(A·2)}$$

The retardation angle of the sublayer is given by

$$\sigma = \frac{\pi}{\lambda}\frac{d}{\cos\alpha}\Delta n\sin^2\psi, \qquad \text{(A·3)}$$

with λ the wavelength of the light, Δn the birefringence, d the thickness of the birefringent layer, and ψ the angle between the director **n** and the wavevector **k**. The term $\Delta n\sin^2\psi$ represents the effective birefringence for the orientation of **n** relative to **k**, whereas the term $d/\cos\alpha$ represents the distance traveled by the light upon passing the sublayer. The angle ψ is given by

$$\cos\psi = \sin\alpha\,\cos\theta\,\cos\phi + \cos\alpha\,\sin\theta. \qquad \text{(A·4)}$$

Figure A·1 shows the relevant vectors and angles. The Jones matrix J_{sublayer} of the sublayer can now be expressed in the general form (5) with

$$a = \cos\sigma + i\cos(2\chi)\sin\sigma, \qquad \text{(A·5a)}$$

$$b = i\sin(2\chi)\sin\sigma. \qquad \text{(A·5b)}$$

The reflections at the air/glass interfaces are taken into account by the attenuation coefficient R, given by:

$$R = \left(t_p^2\sin^2\xi_1 + t_s^2\cos^2\xi_1\right)\left(t_p^2\sin^2\xi_2 + t_s^2\cos^2\xi_2\right). \qquad \text{(A·6)}$$

Here ξ_1 and ξ_2 are the angles between the p-polarization and the polarizations transmitted by the polarizer and analyzer, respectively. The coeficients t_p and t_s are the Fresnel coefficients of the p and s polarized waves for the air/glass interface. They can be expressed as

$$t_p = \frac{2\sqrt{n_{\text{air}}n_{\text{glass}}\cos\alpha_{\text{air}}\cos\alpha_{\text{glass}}}}{n_{\text{air}}\cos\alpha_{\text{glass}} + n_{\text{glass}}\cos\alpha_{\text{air}}}, \qquad \text{(A·7a)}$$

$$t_s = \frac{2\sqrt{n_{\text{air}}n_{\text{glass}}\cos\alpha_{\text{air}}\cos\alpha_{\text{glass}}}}{n_{\text{air}}\cos\alpha_{\text{air}} + n_{\text{glass}}\cos\alpha_{\text{glass}}}, \qquad \text{(A·7b)}$$

with n_{air} and n_{glass} the refractive indices of air and glass, respectively, and α_{air} and α_{glass} the angles between the normal to the interfaces and the light ray in air and glass, respectively. These angles and refractive indices are related by Snel's law:

$$n_{\text{air}}\sin\alpha_{\text{air}} = n_{\text{glass}}\sin\alpha_{\text{glass}}. \qquad \text{(A·8)}$$

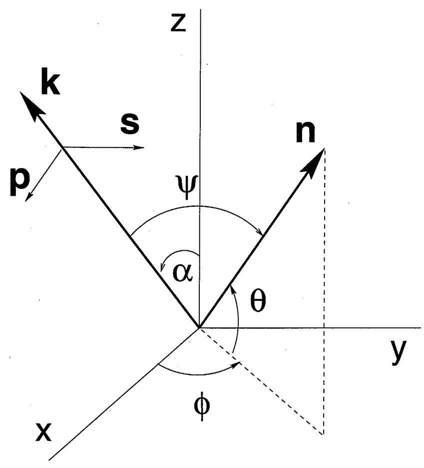

Fig. A·1. The relative orientation of the wavevector **k** and director **n** in the xyz-coordinate frame. The xz-plane is taken to be the plane of incidence.

1) M. Schadt and W. Helfrich: Appl. Phys. Lett. **18** (1971) 127.
2) H. Mori, Y. Itoh, Y. Nishiura, T. Nakamura and Y. Shinagawa: AM-LCD '96/IDW '96 Dig. p. 189.
3) H. Mori, Y. Itoh, Y. Nishiura, T. Nakamura and Y. Shinagawa: Jpn. J. Appl. Phys. **36** (1997) 143.
4) P. van de Witte, S. Stallinga and J. A. M. M. van Haaren: SID '97 Dig. (1997) p. 687.
5) J. P. Eblen Jr., L. G. Hale, B. K. Winkler, D. B. Taber, P. Kobrin, W. J. Gunning III, M. C. Skarohlid, T. A. Seder, J. D. Sampica and P. M. Franzen: SID '97 Dig. (1997) p. 683.
6) M. Oh-e and K. Kondo: Appl. Phys. Lett. **26** (1995) 3895.
7) M. Oh-e and K. Kondo: Appl. Phys. Lett. **69** (1996) 623.
8) M. Oh-e and K. Kondo: Liq. Cryst. **22** (1997) 379.
9) S. Kaneko, Y. Hirai and K. Sumiyoshi: SID '93 Dig. (1993) p. 265.
10) T. Sugiyama, Y. Toko, T. Hashimoto, K. Katoh, Y. Iimura and S. Kobayashi: SID '94 Dig. (1994) p. 915.
11) N. Yamada, S. Kohzaki and F. Funuda: SID '95 Dig. (1995) p. 575.
12) S. Kohzaki, N. Yamada, Y. Ishii, F. Funuda and K. Awane: SID '96 Dig. (1996) p. 630.
13) K. Ohmuro, S. Kataoka, T. Sasaki and Y. Koike: SID '97 Dig. (1997) p. 845.
14) T. Miyashita, C.-L. Kuo, M. Suzuki and T. Uchida: SID '95 Dig. (1995) p. 797.
15) S. Zimmerman, M. McFarland, J. Wilson, T. J. Credelle, K. Bingaman, P. Ferm and J. T. Yardley: SID '95 Dig. (1995) p. 793.
16) R. C. Jones: J. Opt. Soc. Am. **31**(1941) 488.
17) P. Yeh: J. Opt. Soc. Am. **72** (1982) 507.
18) C. Gu and P. Yeh: J. Opt. Soc. Am. **10** (1993) 966.
19) A. Lien: Appl. Phys. Lett. **57** (1990) 2767.
20) D. W. Berreman: J. Opt. Soc. Am. **62** (1972) 502.
21) H. Wöhler, G. Haas, M. Fritsch and D. A. Mlynski: J. Opt. Soc. Am. A **5** (1988) 1554.
22) K. Eidner, G. Mayer, M. Schmidt and H. Schmiedel: Mol. Cryst. Liq. Cryst. **172** (1989) 191.
23) C. Oldano: Phys. Rev. A **40** (1989) 6014.
24) H. A. van Sprang: J. Appl. Phys. **71** (1992) 4826.
25) J. E. Bigelow and R. A. Kashnow: Appl. Opt. **16** (1977) 2090.
26) A. De Meyere: J. Opt. Soc. Am. A **11** (1994) 731.
27) H. Yoshida and J. R. Kelly: Jpn. J. Appl. Phys. **36** (1997) 2116.
28) H. A. van Sprang: Mol. Cryst. Liq. Cryst. **199** (1991) 19.
29) M. Nishikawa, T. Miyamoto, S. Kawamura, Y. Tsuda and N. Bessho: IDRC '92 Dig. (1992) p. 819.